The EUV Coronae of the Young Solar Analogs 47 Cas & EK Dra: An EUVE Spectroscopic and Timing Study of Coronal Heating

Marc Audard[1] and Manuel Güdel[1]
Paul Scherrer Institute, Würenlingen & Villigen, 5232 Villigen PSI, Switzerland,
audard@astro.phys.ethz.ch, guedel@astro.phys.ethz.ch

and

Edward F. Guinan
Department of Astronomy & Astrophysics, Villanova University, Villanova, PA 19085, USA,
guinan@ucis.vill.edu

ABSTRACT

We present results of an EUV spectroscopic and timing study of one of the most active main-sequence stars, 47 Cas B. EUVE observed the system for almost 7 days. A number of emission lines were clearly detected in the SW spectrometer, including lines of Fe at ionization stages between Fe XV and Fe XXIII that could be used to derive the coronal EM distribution. We performed 2 and 3 temperature fits using the CIE models implemented in the Utrecht SPEX software. We found that a low hydrogen column density $N_{\rm H}$ ($\sim 10^{18}$ cm^{-2}) was required to fit the combined SW-MW spectrum. The 3-T CIE model gave an Fe abundance of 0.28 times solar photospheric. This value is quite different from iron abundances obtained for several other G stars (often around 0.8). Different reconstruction methods for emission measure distributions showed no significant coronal emission at low temperatures ($kT < 0.3$ keV). The EM distribution was found to be bi-modal, with two peaks at ~ 0.5 keV and ~ 1.3 keV.

We then performed a timing analysis of the EUVE Deep Survey light curves of 47 Cas B and the similar solar analog EK Dra. Fourier transform, autocorrelation and structure function were used to test the presence of a rotational modulation period and to characterize the statistical properties of the considerable flare variability. A test based on different time-phasing of the light curve was then applied. We characterized bin count rates in terms of the probability for flaring emission. The detected flares were used to investigate the flare distribution in energy. We derived power-law indices suggesting a considerable contribution of small energy flares to the coronal heating of these two stars.

1. Introduction

Late-type stars are prominent sources of magnetic coronal activity as seen in the X-ray, the EUV and the radio domains. The Extreme Ultraviolet Explorer (EUVE, Malina & Bowyer 1991)

[1]also at Institute of Astronomy, ETH Zentrum, 8092 Zürich, Switzerland

has been pioneering the EUV domain. Numerous spectroscopic studies were performed with the three spectrometers on board EUVE (see, e.g., Schmitt et al. 1996). The Deep Survey Photometer (67-178 Å) imaging data were often used to display light curves in order to derive parameters of coronal loops (from duration, rise & decay times, luminosity at maximum). However, a general study of light curve variability and flare distribution statistics has yet to be performed. EUVE is an excellent observatory for this purpose as very long contiguous observations are available (several days). This kind of analysis is important to help clarifying the 'microflare hypothesis': solar flares have been found to be distributed in energy according to a power-law, i.e., $dN/dE \propto E^{-\alpha}$, with $\alpha \approx 1.5 - 2.5$. If $\alpha \gtrsim 2$, the probability exists that an extrapolation to lower energies may provide the energy necessary to heat the complete corona (see, e.g., Hudson 1991).

2. Observations and Data Reduction

2.1. 47 Cas & EK Dra

47 Cas is a F0V main-sequence star, probably coeval with the Pleiades. Hipparcos revealed its binary origin (Güdel et al. 1998). The secondary star (47 Cas B) is thought to be a dG star, invisible in the optical range but very luminous in EUV, X-rays and radio, while the optical primary star is dark in these ranges. Hipparcos determined a distance of 33.6 pc. The EUVE observation was part of the Guest Observer Program and lasted almost 7 contiguous days. A short ($5^{\rm h}40^{\rm m}$) gap in the last part of the observation was due to an ALEXIS target of opportunity observation.

We used events and image FITS files from the EUVE Archive. Standard data reduction was performed. For the spectral analysis, we only used the SW and MW spectrometer data only, since no obvious lines were visible in the LW data. We used the DS data to extract a light curve (Fig. 1a) with a binsize of the order of the orbital period of EUVE ($96^{\rm m}$). A circle for the source and a concentric annulus for the background were defined before the extraction of the counts.

We extended our timing study to another very active young solar analog, EK Dra. EUVE spectral analysis and a complete description of the star is found in Güdel et al. (1997). Although the photon DS image was found to lie near the dead spot, we carefully analyzed the positions of the detected events in detector coordinates to conclude that there was no significant effect on the light curve variability.

3. The Spectrum of 47 Cas

We analyzed the extracted spectrum of 47 Cas with the Utrecht Software SPEX (Kaastra, Mewe, & Nieuwenhuijzen 1996). We rebinned the original spectrum by a factor of 8 in order to obtain a resolution almost equal to the EUVE spectrometers' resolutions (0.5 Å and 1 Å for the SW & MW, respectively), leading to a total of 385 data channels after removing bad channels and channels close to the He II λ303.78 line. Figure 1b shows the combined spectrum on a logarithmic wavelength scale. The MW spectrum is plotted with a shift of $-5 \cdot 10^{-4}$ counts $\cdot\, {\rm s}^{-1} \cdot {\rm Å}^{-1}$ for illustration. Several iron lines with ionization stages from Fe XV to Fe XXIII were detected,

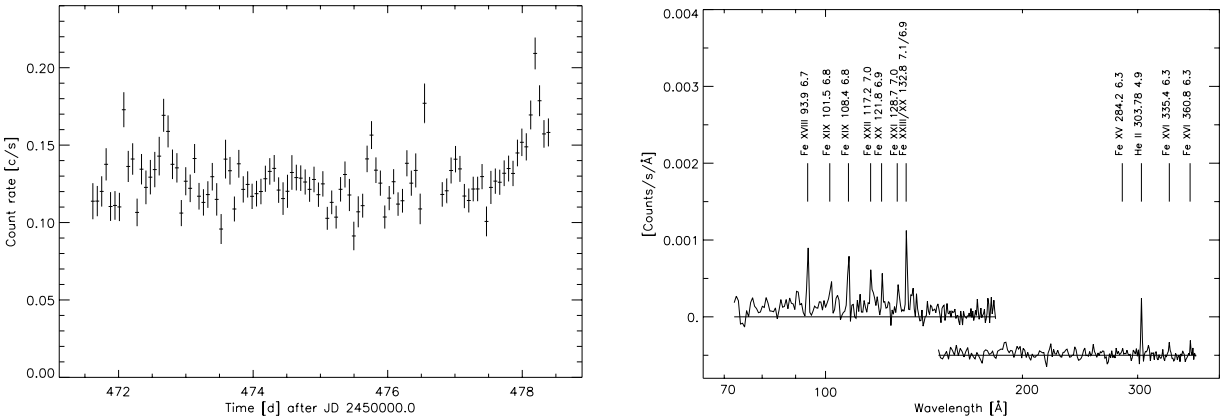

Fig. 1.— (a) 47 Cas: DS light curve; (b) SW/MW spectrum.

implying line formation temperatures ranging from $10^{6.3}$ to $10^{7.0}$ K.

We used the collisional ionization equilibrium (CIE) in SPEX together with an hydrogen absorption component to determine the element abundances and the hydrogen column density $N_{\rm H}$. Two and three temperature fits were performed. The 3-T CIE model with the third temperature restricted to less than 0.3 keV gave a good fit, with an iron abundance around 0.3 times the solar photospheric value. A low $N_{\rm H}$ value (10^{18} cm^{-2}) was required to fit the combined SW-MW spectrum. We then performed a polynomial DEM fit to the spectrum, using Chebychev polynoms. Two bumps appeared for different polynomial degrees. Therefore, we next applied a 2-T CIE model fit, with $N_{\rm H}$ fixed and the iron abundance free. Again, an acceptable fit yielded Fe ~ 0.3. Finally, using both the updated iron abundance and fixed $N_{\rm H}$ we applied three different DEM methods: Chebychev polynoms, regularization inversion and CLEAN algorithm (see Audard et al. 1998 for further details).

4. A Timing Study

4.1. Method

Our light curve analysis method is derived from the method that Robinson et al. (1995) presented for UV studies. Only pivotal points are summarized here. We first defined a 'quiescent' emission by excluding photon arrival times that belong to obvious flaring intervals. We then binned these to a small binsize ($\frac{1}{50}$ of $96^{\rm m}$) in order to obtain a sufficient number of counts per bin. Next, we used these 'original bins' to test if a Poisson distribution could describe the 'quiescent' emission, for different binsizes. Figure 2, top panel, shows the resulting distribution for a binsize of the order of the satellite orbital period. The derived Poissonian distribution is superimposed. As this method is 'phase' dependent, we tested the distribution with several reference phases and took the largest number of counts in the bin to derive the final distribution (Fig. 2, bottom panel, see Audard et al. (1998) for details). The new distribution is no longer fitted by a Poisson distribution. It was used to assign an occurence probability to each measured number of counts.

Using the complete data, we binned the photon arrival times at different binsizes and different reference phases. Knowing for a particular binsize the true number of counts in the bins, we used the time-phased quiescent counts distribution to derive the probabilities for the presence of 'quiescent-only' emission.

4.2. 47 Cas

Figure 3 shows the resulting 'significance plot' after excluding probabilities higher than 10^{-3} for quiescence and counts per bin less than the mean value of the distribution, thus leading to a plot showing only significant 'flares'. Very small probabilities (dark grey) characterize very probable 'flares' while higher probabilities (light grey) indicate less probable flaring events. We excluded a detection just before the TOO, as the end of the flare could not be determined. To determine timing characteristics of the flares, we used a smoothed 'background' light curve (Fig. 4a). Gaussian fits were performed to determine the flare durations, their beginnings and aproximate ends. Due to its peculiar shape, the parameters of the last flare were determined by eye.

The timing and spectral (EM) characteristics allowed us to determine the total X-radiated energy of a flare as well as the cumulative flare energy distribution. We refer to Audard et al. (1998) for details. The conversion factor between counts and energy was determined from the DEM polynomial fit. We obtained a value of $2.5 \cdot 10^{30}$ ergs $\cdot$ s^{-1} over the total X-ray regime for a weighted mean DS count rate of 0.1267 counts/s, which yielded a conversion factor of $1.97 \cdot 10^{31}$ ergs per count. Figure 4b shows the cumulative flare distribution in total energy. We fitted a power-law function, without error bars. Three different results were derived, depending on the in- or exclusion of the last point and of the first three points (near the detection threshold). The indices are almost identical. X-ray solar flare cumulative distributions give almost the same indices

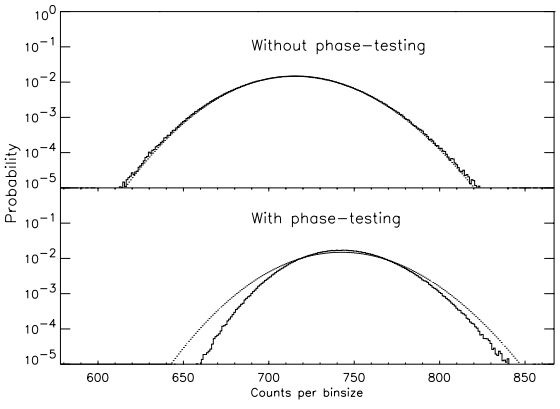

Fig. 2.— Count distributions for a binwidth of 96 min with and without phase-testing.

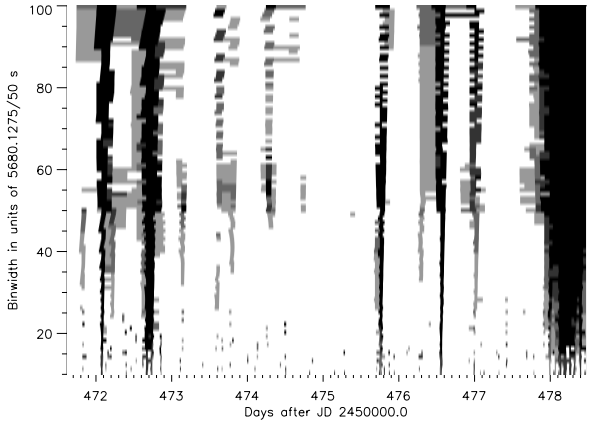

Fig. 3.— 'Significance plot' for 47 Cas as a function of time and binwidth.

(e.g. Crosby et al. 1993).

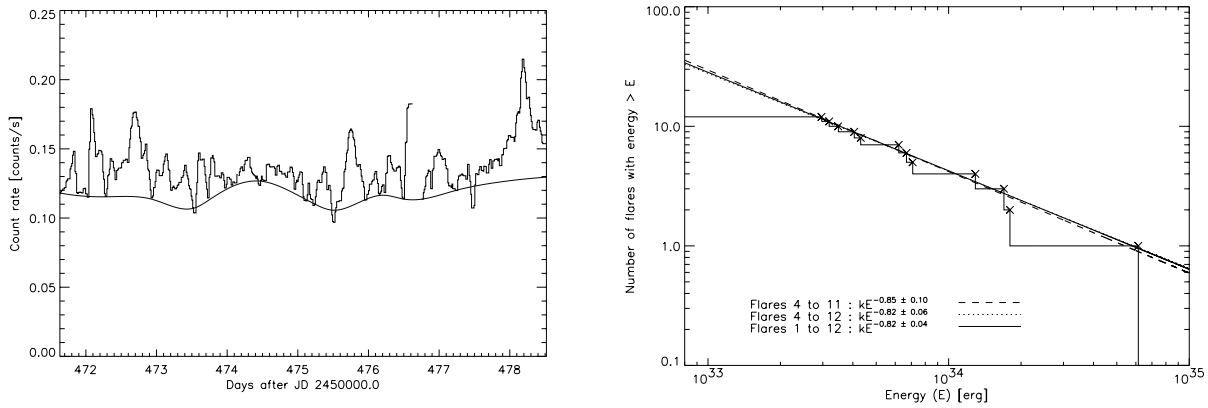

Fig. 4.— (a) 47 Cas: median smoothed light curve and smoothed lower envelope; (b) cumulative flare distribution in total energy.

4.3. EK Dra

EK Dra's light curve (Güdel et al. 1997) displays very frequent and long-lasting flares. Due to the large activity, the short 'quiescent' intervals were not sufficient to derive efficiently the count distributions. We therefore simulated a 'quiescent emission', using the level of the quiescent data. Figure 5a displays the 'significance plot'. 17 flares are extracted. Fig. 5b shows the cumulative flare distribution for EK Dra. The conversion factor was $2.1 \cdot 10^{31}$ ergs per count. The distribution is not precisely a power-law within the low and high energy parts. This is mainly due to large inherent energy error bars for the former and the uncertainty in the occurence rate of large flares. Nevertheless, excluding the 'uncertain' parts, we retrieve a power-law index significantly higher than for 47 Cas. This might indicate a much greater contribution of low-energetic flares, suggesting that a considerable portion of the coronal energy release may be provided by flares.

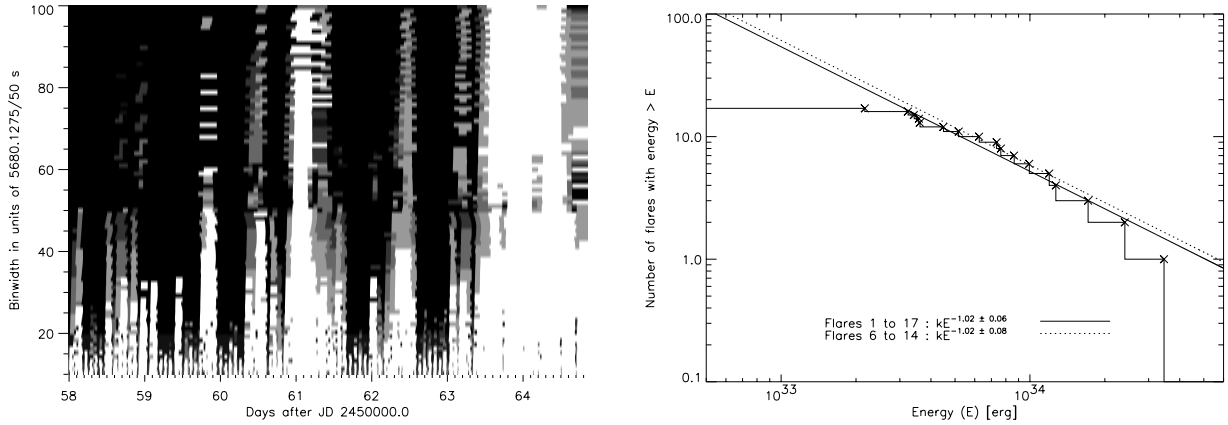

Fig. 5.— (a) EK Dra: 'significance plot'; (b) cumulative flare distribution in total energy.

5. Conclusion

We analyzed data from the EUVE observations of 47 Cas. We showed that many iron lines were present, from ionization stages XV to XXIII. Final multi-temperature CIE and DEM methods fits yielded an interstellar hydrogen column density $N_{\rm H}$ of 10^{18} cm^{-2} and an iron abundance of 0.3 times the solar photospheric value, resulting in a two-bump differential emission measure distribution. The average X-ray luminosity was derived and allowed us to calculate a conversion factor between energy and counts.

We applied a timing method originally presented by Robinson et al. (1995) and modified by us for characterizing flares, in order to determine the cumulative flare distribution in total energy. This distribution was fitted with a power-law and yielded indices comparable to solar. We also studied the DS observation of EK Dra. The power-law index suggested a larger contribution of small flares. This result may indicate that coronal flares are largely responsible for the coronal heating in young active stars. We are presently studying important corrections to the flare distribution due to overlapping flares; the analysis is being extended to other EUVE data sets (Audard et al. 1998).

Marc Audard acknowledges support from the Swiss National Science Foundation, grant 21-49343.96. He also thanks for help from the CEA EUVE team.

REFERENCES

Audard, M., Güdel, M., Guinan, E. F. 1998, ApJ, in preparation

Crosby, N. B., Aschwanden, M. J., & Dennis, B. R. 1993, Sol. Phys., 143, 275

Güdel, M., Guinan, E. F., Mewe, R., Kaastra, J. S., & Skinner, S. L. 1997, ApJ, 479, 416

Güdel, M., Guinan, E. F., Etzel, P. B., et al. 1998, in The Tenth Cambridge Workshop on Cool Stars, Stellar Systems and the Sun, eds. R. A. Donahue & J. A. Bookbinder (San Francisco: ASP), 1247

Hudson, H. S. 1991, Sol. Phys., 133, 357

Kaastra, J. S., Mewe, R., & Nieuwenhuijzen, H. 1996, in UV and X-ray Spectroscopy of Astrophysical and Laboratory Plasmas, eds. K. Yamashita & T. Watanabe (Tokyo: Univ. Acad. Press), 411

Malina, R. F., & Bowyer, S. 1991, in Extreme Ultraviolet Astronomy, ed. R. F. Malina & S. Bowyer (New York: Pergamon), 397

Robinson, R. D., Carpenter, K. G., Percival, J. W., & Bookbinder, J. A. 1995, ApJ, 451, 795

Schmitt, J. H. M. M., Drake, J. J., Stern, R. A., & Haisch, B. M. 1996, ApJ, 457, 882

This preprint was prepared with the AAS LaTeX macros v4.0.